Biomaterials 30 (2009) 4877–4888

Contents lists available at ScienceDirect

Biomaterials

journal homepage: www.elsevier.com/locate/biomaterials

pH-triggered injectable hydrogels prepared from aqueous *N*-palmitoyl chitosan: *In vitro* characteristics and *in vivo* biocompatibility

Ya-Ling Chiu [a], Sung-Ching Chen [b], Chun-Jen Su [c], Chun-Wen Hsiao [a], Yu-Ming Chen [a], Hsin-Lung Chen [a,**], Hsing-Wen Sung [a,*]

[a] *Department of Chemical Engineering, National Tsing Hua University, Hsinchu 30013, Taiwan, ROC*
[b] *Biomaterial Application Lab, Biomedical Engineering Research Laboratories, Industrial Technology Research Institute, Hsinchu, Taiwan, ROC*
[c] *National Synchrotron Radiation Research Center (NSRRC), Hsinchu, Taiwan, ROC*

ARTICLE INFO

Article history:
Received 28 March 2009
Accepted 21 May 2009
Available online 13 June 2009

Keywords:
pH-sensitive hydrogel
N-Palmitoyl chitosan
Viscoelastic property
Biocompatibility

ABSTRACT

In-situ forming hydrogels triggered by environmental stimuli have emerged as a promising injectable strategy targeted for various biomedical applications. However, several drawbacks associated with temperature-stimulated hydrogels have been reported. Employing a hydrophobically-modified chitosan (*N*-palmitoyl chitosan, NPCS), we developed a pH-triggered hydrogel system which showed a rapid nanostructure transformation within a narrow pH range (pH 6.5–7.0). NPCS in an aqueous environment was found to be a shear-thinning fluid and exhibited an instant recovery of its elastic properties after shear thinning, thereby making it an injectable material. Additionally, aqueous NPCS, an associating polyelectrolyte, can be rapidly transformed into hydrogel triggered simply by its environmental pH through a proper balance between charge repulsion and hydrophobic interaction. This *in-situ* hydrogel system was shown to be nontoxic. Subcutaneous injection of aqueous NPCS (pH 6.5) into a rat model resulted in rapid formation of a massive hydrogel at the location of injection. The implanted hydrogel was found to be degradable and was associated with an initial macrophage response which decreased with time as the degradation proceeded. These results suggested that the developed NPCS hydrogel may be used as an injectable drug/cell delivery system.

1. Introduction

Polymer solutions that can be transformed into hydrogels *in situ*, as a result of changes in environmental conditions, have attracted the attention of many investigators for scientific interest [1,2]. Prior to hydrogelation, bioactive molecules or cells can be readily mixed with polymer solutions, thus allowing for practical pharmaceutical or tissue-engineering applications. Additionally, formation of hydrogel *in situ* enables the preparation of complex shapes in the human body and the use of minimally invasive surgery [3,4].

Temperature-sensitive hydrogels have been comprehensively investigated in the literature [5]. Premature hydrogelation and blockage of a needle, especially a catheter, during the injection of hydrogel precursors into deep anatomical sites in the body limits their applications [6–8]. Additionally, diffusion of polymer solutions into the surrounding tissue has been reported [9,10]. To overcome these problems, we focus on developing a pH-triggered hydrogel system which shows a rapid nanostructure transformation within a narrow pH range, using a naturally-abundant biopolymer, chitosan (CS), conjugated with hydrophobic side chains.

Considering that the pK_a of CS is 6.0–6.5 [11], a pH-triggered hydrogelation may take place when it is brought to the physiological pH of approximately 7.4. However, in our preliminary study [12], CS was found to form dissociated precipitates rather than a massive hydrogel at pH > 6.2. To enhance the intermolecular contact of CS molecules while retaining their pH sensitivity, a hydrophobic palmitoyl group is conjugated onto the free amine groups of CS to produce a comblike associating polyelectrolyte, *N*-palmitoyl CS (NPCS). Through a proper balance between charge repulsion and hydrophobic interaction, this associating polyelectrolyte can undergo a rapid hydrogelation triggered simply by its environmental pH within a narrow range. The transition of hydrogelation is accomplished in an aqueous environment, eliminating the need of harmful organic solvents or toxic polymerization agents.

* Corresponding author. Tel.: +886 3 574 2504; fax: +886 3 572 6832.
** Corresponding author.
E-mail addresses: hlchen@che.nthu.edu.tw (H.-L. Chen), hwsung@che.nthu.edu.tw (H.-W. Sung).

0142-9612/$ – see front matter © 2009 Elsevier Ltd. All rights reserved.
doi:10.1016/j.biomaterials.2009.05.052

In the study, the synthesized NPCS was analyzed by the proton nuclear magnetic resonance (^{1}H NMR) and Fourier transformed infrared (FT-IR) spectroscopy. Rheology experiments were performed to investigate the viscoelastic properties of aqueous NPCS at different pH, temperature, and shear rate environments. The morphology of the formed hydrogel was examined by small-angle X-ray scattering (SAXS) and scanning electron microscopy (SEM) and transmission electron microscopy (TEM). Additionally, the cytotoxicity of the hydrogel was studied *in vitro* and its *in vivo* compatibility/degradability was inspected in a rat model subcutaneously.

2. Materials and methods

2.1. Materials

CS (viscosity 36 mPa s, 0.5% in 0.5% acetic acid at 20 °C, MW 500 kDa) with a degree of deacetylation of approximately 85% was purchased from Koyo Chemical Co. Ltd. (Tokyo, Japan). Palmitic acid *N*-hydroxysuccinimide ester was obtained from Sigma–Aldrich (St. Louis, MO, USA). All other chemicals and reagents used were of analytical grade.

2.2. Synthesis of NPCS

A mixture of CS (1 g) and aqueous acetic acid (50 mL, 1% w/v) was stirred for 24 h to ensure total solubility. The pH was adjusted to 6.0 by slow addition of 1 N NaOH and the final volume of CS solution was 100 mL. A solution of palmitic acid *N*-hydroxysuccinimide ester (0.3 g) in absolute ethanol was added drop-wise to the CS solution at 98 °C and reacted for 36 h. Subsequently, the prepared solution was cooled at room temperature, added acetone, and precipitated by adjusting its pH value to 9.0. The precipitate (NPCS) was then filtered, washed with an excess of acetone, and air-dried. The synthesized NPCS was analyzed by ^{1}H NMR (Varian Unity Inova 500, Missouri, USA) and FT-IR (Perkin–Elmer Spectrum RX1 System, Buckinghamshire, England).

The degree of substitution on NPCS was determined by the ninhydrin assay [13] and the potassium polyvinylsulfate (PVSK) titration method [14]. For the ninhydrin assay, NPCS (0.3 mg) was dissolved in an aqueous acetic acid (3% w/v, 1 mL) and thoroughly stirred. Subsequently, 0.5 mL of acetic acid/acetate buffer (4 M, pH 5.5) was added into 0.5 mL of the prepared NPCS solution. Ninhydrin regent (1 mL) was then added and test tubes were placed in a boiling water bath for 20 min. The solutions were cooled and their absorbance at 570 nm was read. The acetic acid/acetate buffer was used as a blank and the unmodified CS solution was used as a control.

For the PVSK titration method, NPCS (0.5 g) was dissolved in an aqueous acetic acid (5% w/v, 99.5 g). Subsequently, 30 mL of deionized (DI) water was added into 1 g of the prepared NPCS solution and thoroughly stirred and two drops of 0.1% aqueous toluidine blue was added. The mixed solution was titrated directly with a polyanionic titrant (PVSK) to an indicator end point. The unmodified CS solution was used as a control.

2.3. Rheology study

Rheology experiments were performed with a rheometer (Haake RS 600, Paramus, New Jersey, USA), equipped with a parallel plate (20 mm plate diameter). The viscoelastic properties of aqueous NPCS (1% w/w) at different pH values were monitored via frequency sweep measurements at a fixed strain amplitude of 1% (linear viscoelastic region) to measure the elastic (G') and viscous (G'') moduli. Dynamic frequency spectra were obtained in the linear viscoelastic regime of test samples, as determined by dynamic strain sweep experiments.

The influence of temperature on G' and G'' was investigated via temperature sweep measurements over a temperature range of 4–50 °C at a ramp rate of 0.038 °C/s, an oscillatory strain amplitude of 1%, and a frequency of 0.1 Hz. For shear-thinning studies (network destruction), viscosity was monitored as a function of strain rate. Gel recovery (network restoration, after 1000% strain applied for 180 s) was monitored by observing G' and G'' at a constant frequency of 0.1 Hz as a function of time.

2.4. Hydrogel strength

An amount of 2 mL of aqueous NPCS (1% w/w, pH 6.5) was injected through a needle into a shallow dish. The injected viscous solution in the dish was then immersed into a buffer solution at predetermined pH and ionic-strength values (0, 0.10, 0.15, or 0.30 M NaCl) for 48 h to form hydrogel. The gel strengths (G' and G'') of the hydrogel prepared at different pH and ionic-strength values were determined via frequency sweep measurements at a fixed strain amplitude of 1%.

2.5. Morphological characterization of NPCS hydrogel

SAXS was employed to resolve the transformation of the nanostructure associated with the hydrogelation. The experiments were performed using the BL17B3 beamline at the National Synchrotron Radiation Research Center (NSRRC), Hsinchu, Taiwan. The energy of beam source was 8 keV and its corresponding wavelength λ was 1.55 Å. The scattering intensity was collected using a two-dimensional MarCCD detector with 512×512 pixel resolution. The sample-to-detector distance was 1734.9 mm. The intensity profile was output as the plot of the scattering intensity (I) vs. the scattering vector, $q = (4\pi/\lambda)\sin(\theta/2)$ (θ = scattering angle). The SAXS profiles were corrected for the absorption, the air scattering, and the background arising from thermal diffused scattering.

The morphology of the hydrogel was also examined in real space by SEM and TEM. Lyophilized samples were placed on double-sided tapes, sputter coated with gold and observed by SEM (Model JSM-5600, JEOL Technics, Tokyo, Japan). The ultrathin section, prepared by microtoming at −100 °C with a Reichert Ultracut E low-temperature sectioning system, for TEM observation was stained by OsO_4, which was a preferential staining agent for the CS backbone [15]. TEM micrographs of test samples were taken by a TEM (JEOL-2100, Akishima, Tokyo, Japan) operated at 200 kV.

2.6. In vitro assay

To demonstrate the rapid hydrogelation triggered by pH, aqueous NPCS (1% w/v) at pH 6.5 was loaded in a syringe and subsequently injected through a needle into a physiological saline solution (pH 7.4) at 37 °C. The cytotoxicity of CS precipitates and NPCS hydrogels was evaluated using the elution test method [16,17]. Extracts were obtained by placing CS precipitates or NPCS hydrogels in separate cell culture media (20 mg/mL) in an incubator for 72 h. Each fluid extract obtained was then applied for cell culture. Mouse 3T3 fibroblasts (ATCC CCL-92) were seeded in 12-well plates at 1×10^4 cells/well and were allowed to adhere overnight. The culture medium was subsequently replaced with a fresh one (control) or a fresh one containing extracts derived from CS precipitates or NPCS hydrogels. The cultures were then returned to the incubator and periodically removed for microscopic examination. The viability of cells was qualitatively evaluated according to a live/dead assay using calcein-AM and ethidium homodimer (Molecular Probes # L3224, Eugene, Oregon, USA) [18] and quantitatively determined by the MTT assay [19].

2.7. In vivo study

Animal care and use was performed in compliance with the "Guide for the Care and Use of Laboratory Animals" prepared by the Institute of Laboratory Animal Resources, National Research Council, and published by the National Academy Press, revised 1996 and approved by the institutional review board (IRB, National Tsing Hua University, Hsinchu, Taiwan). Wistar rats (250–300 g) were used in the study. Rats were anesthetized using pentobarbital prior to experiment. After shaving and disinfection, 500 μL of the sterilized aqueous NPCS (1% w/v, pH 6.5) was injected subcutaneously (Fig. 1). At predetermined periods, rats were sacrificed and the hydrogel and its surrounding tissue were isolated. For histological examination, samples were fixed in 4% neutral buffered formalin and then stained with hematoxylin–eosin (H&E) using standard techniques.

Additional sections were investigated using the immunohistochemical stains to identify the inflammatory cells populated in the subcutaneous tissue and hydrogel. The antibody used in the study was monoclonal mouse anti-rat CD68 (AbD Serotec, Oxford, UK). The stained sections were counterstained to visualize nuclei by propidium iodide (PI, Sigma–Aldrich, USA) and examined using an inverted confocal laser scanning microscope (CLSM, TCS SL, Leica, Germany).

2.8. Statistical analysis

Comparison between two groups was analyzed by the one-tailed Student's t-test using statistical software (SPSS, Chicago, IL, USA). Data are presented as mean ± SD. A difference of $P < 0.05$ was considered statistically significant.

3. Results and discussion

Hydrophobically-modified CS has been prepared previously for developing drug delivery vehicles such as micro-particles, nanoparticles, and tablets [20–22]. It was reported that hydrophobic side chains can be attached to the CS backbone by reacting CS with long-chain acyl chlorides or anhydrides in an aqueous environment [23]. However, acyl chlorides or anhydrides may also react with water rigorously, thus causing an uncontrollable degree of substitution and producing undesired by-products [24]. Hydrophobically-modified CS can also be prepared via the reaction of the amine groups on CS with alkyl aldehydes; the produced imine groups are subsequently

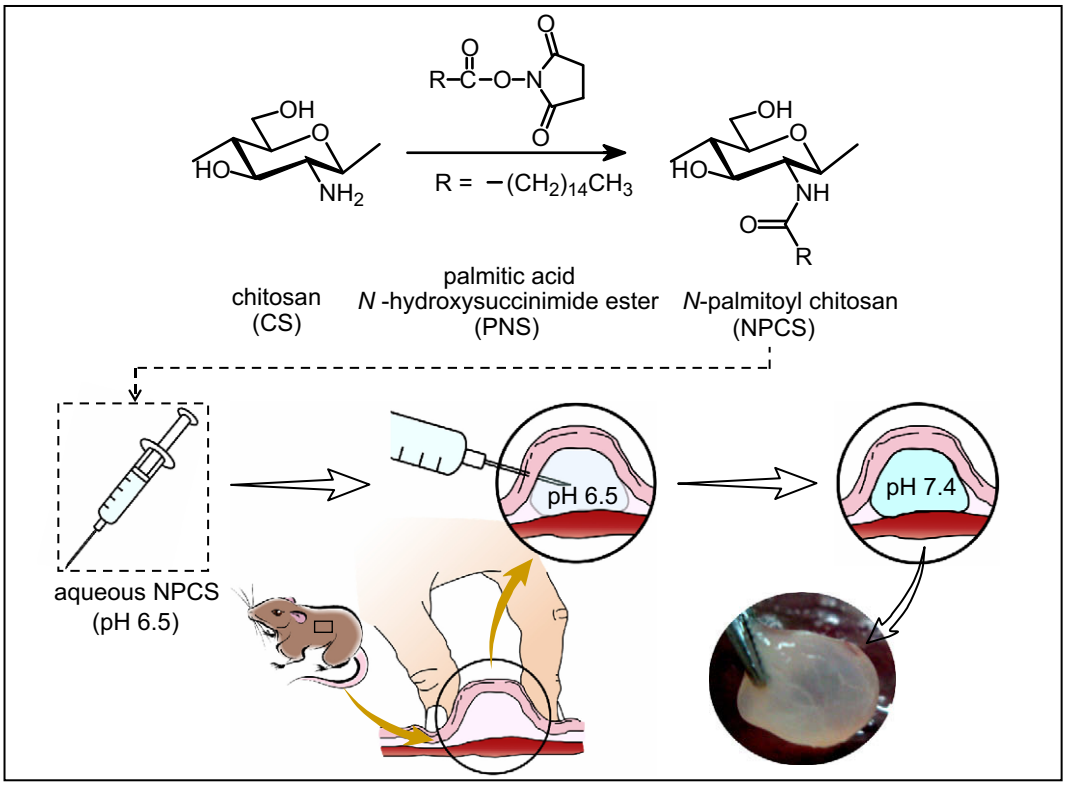

Fig. 1. Schematic illustrations of the synthesis of *N*-palmitoyl chitosan (NPCS) and the pH-triggered hydrogelation of aqueous NPCS which was injected through a needle into the subcutaneous space of a rat model.

reduced by sodium cyanohydroborate [25]. Nevertheless, this synthetic method led to a relatively low degree of substitution of 1–5% [26–30]. Due to the lack of sufficient hydrophobic interaction between the modified CS molecules with a low degree of substitution, their hydrogelation has never been realized before.

In the present study, we employed a method which was able to produce NPCS with a relatively high and controllable degree of substitution. The synthesis was accomplished in a single-step reaction which had been used in forming amide bonds in the synthesis of peptides [31]. Furthermore, with the investigation of the material over a broad range of pH from 3.0 to 8.0, we disclosed a rapid hydrogel transition near the physiological pH.

3.1. Characterization of the synthesized NPCS

Fig. 2a and b shows the ^{1}H NMR and FT-IR spectra of CS and the synthesized NPCS, respectively. As shown in Fig. 2a, NPCS showed a new signal at 0.75 ppm ($-CH_3$), while those observed at 1.1–1.2 ppm corresponded to [$-(CH_2)-$]. Compared to CS, the FT-IR spectrum of NPCS showed an increase in the peak intensities at 1655 cm^{-1} and 1550 cm^{-1}, corresponding to amide bond C═O stretching and N–H bending vibrations, respectively (Fig. 2b). In addition, a characteristic absorption at 2800–2950 cm^{-1} [$-(CH_2)-$] was observed in the spectrum of NPCS. These results indicated that the palmitoyl group was successfully conjugated onto the free amine groups of CS. The degree of substitution on NPCS determined by the ninhydrin assay and the PVSK titration method was 15.1 ± 0.2% and 17.0 ± 0.1%, respectively ($n = 5$).

3.2. Viscoelastic properties of aqueous NPCS

When aqueous CS was dialyzed against DI water using a dialysis tube, local dissociated precipitates were observed at pH > 6.2, while aqueous NPCS remained in a solution state at pH ≦ 6.5 and changed into a massive hydrogel at a higher pH. Additionally, we found that in dilute aqueous solutions, NPCS polymers were able to self-assemble into micelles (observed by a dynamic-light-scattering spectrometer, data not shown) due to the hydrophobic interaction between the conjugated palmitoyl groups. With increasing the polymer concentration, aqueous NPCS showed a thickening property and was able to produce a viscous solution. This viscosity enhancement is due to the strong tendency of its hydrophobic side chains to from intermolecular aggregates, presumably a micellar type [32], which can act as physical cross-links between NPCS polymers.

Fig. 3 displayed the elastic (G') and viscous (G'') moduli of aqueous CS (pH ≦ 6.2) and NPCS (pH ≦ 6.5) measured at a constant frequency of 0.1 Hz as a function of pH. For aqueous CS, G'' was greater than G' ($P < 0.05$), exhibiting a viscous nature, over the entire range of pH values investigated. In the case of aqueous NPCS, G' was found to be approximately an order of magnitude larger than G'' ($P < 0.05$), indicative of an elastic rather than viscous material.

It is known that the charged state and physiochemical properties of CS are substantially influenced by its environmental pH [11,23,33]. At low pH, the free amine groups on CS were protonated ($-NH_3^+$), thus limiting the physical contact between CS molecules due to charge repulsion (Fig. 3b). With increasing pH, the amine groups on CS tended to be deprotonated ($-NH_2$) and hydrogen bonds between the hydroxyl groups and the uncharged amine groups were formed. Therefore, chain entanglements were developed via a simple topological interaction of CS polymers and their dynamic rheologic response reflected a viscous nature over a pH range of 3.0–6.2.

The synthesized NPCS is an associating polymer characterized by the presence of alternating charges (protonated amine groups)

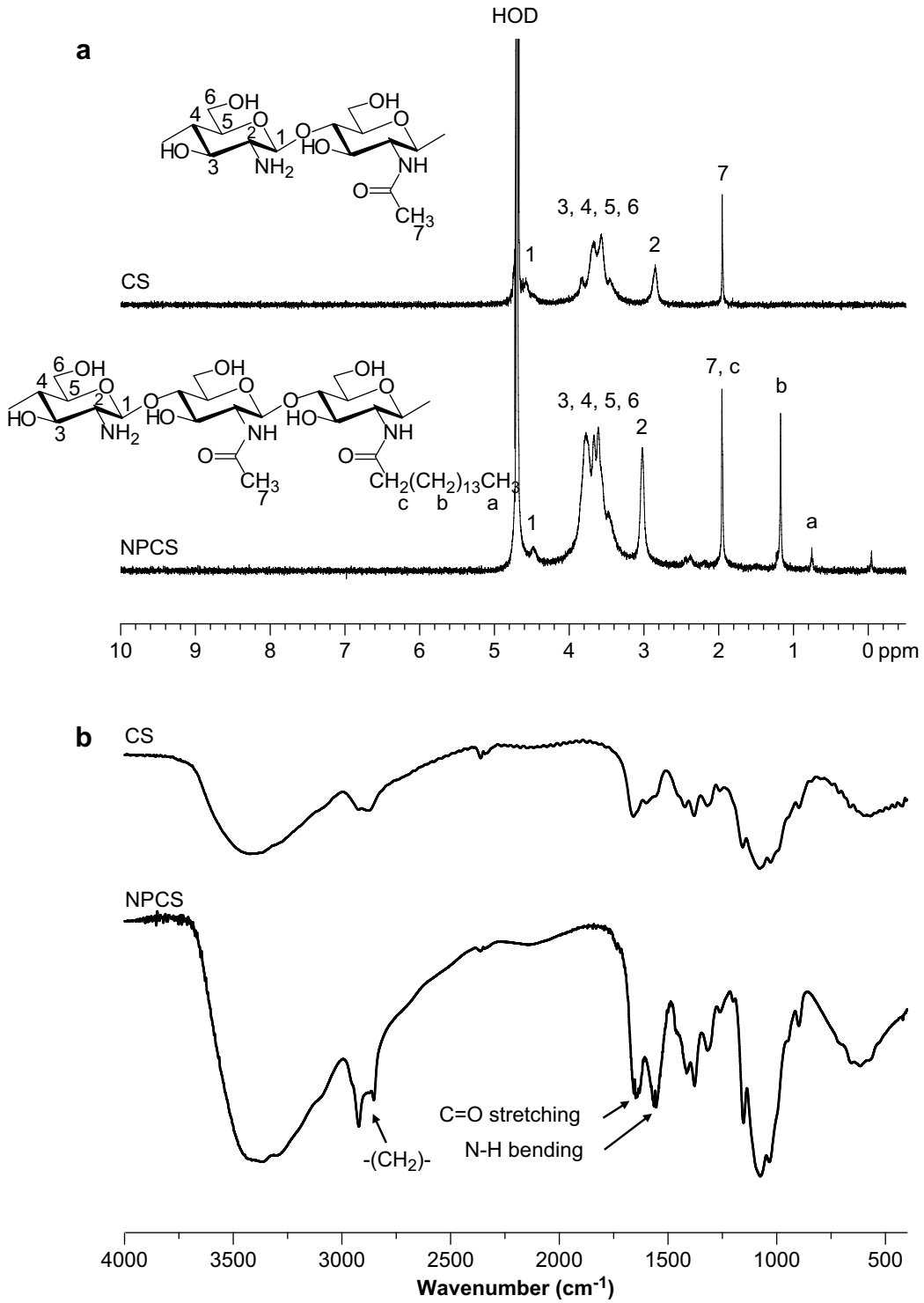

Fig. 2. (a) ^{1}H NMR spectra of chitosan (CS) and *N*-palmitoyl chitosan (NPCS); (b) FT-IR spectra of CS and NPCS.

and hydrophobic side chains (palmitoyl groups). The balance between charge repulsion and hydrophobic interaction on NPCS chains is sensitive to their environmental pH. At low pH, the charge repulsion between the protonated amine groups on NPCS dominated, leading to the extension of polymer chains (Fig. 3b). As pH was increased, the hydrophobic interaction between the palmitoyl groups took the control, causing NPCS polymers to progressively condense and create distinct inter-chain network aggregates (i.e., a significant increase in intermolecular physical cross-links). This led to a substantial increase in G', suggesting an enhancement of the elastic nature of aqueous NPCS. Therefore, NPCS behaves as a polyelectrolyte at low pH and as a polysoap at high pH.

Results of the effect of temperature on the viscoelastic properties of aqueous NPCS (pH 6.5) are presented in Fig. 3c. As shown, the elastic (G') and viscous (G'') moduli of aqueous NPCS remained approximately the same over the entire temperature range investigated (4–50 °C), suggesting that the viscoelastic properties of aqueous NPCS were not sensitive to temperature.

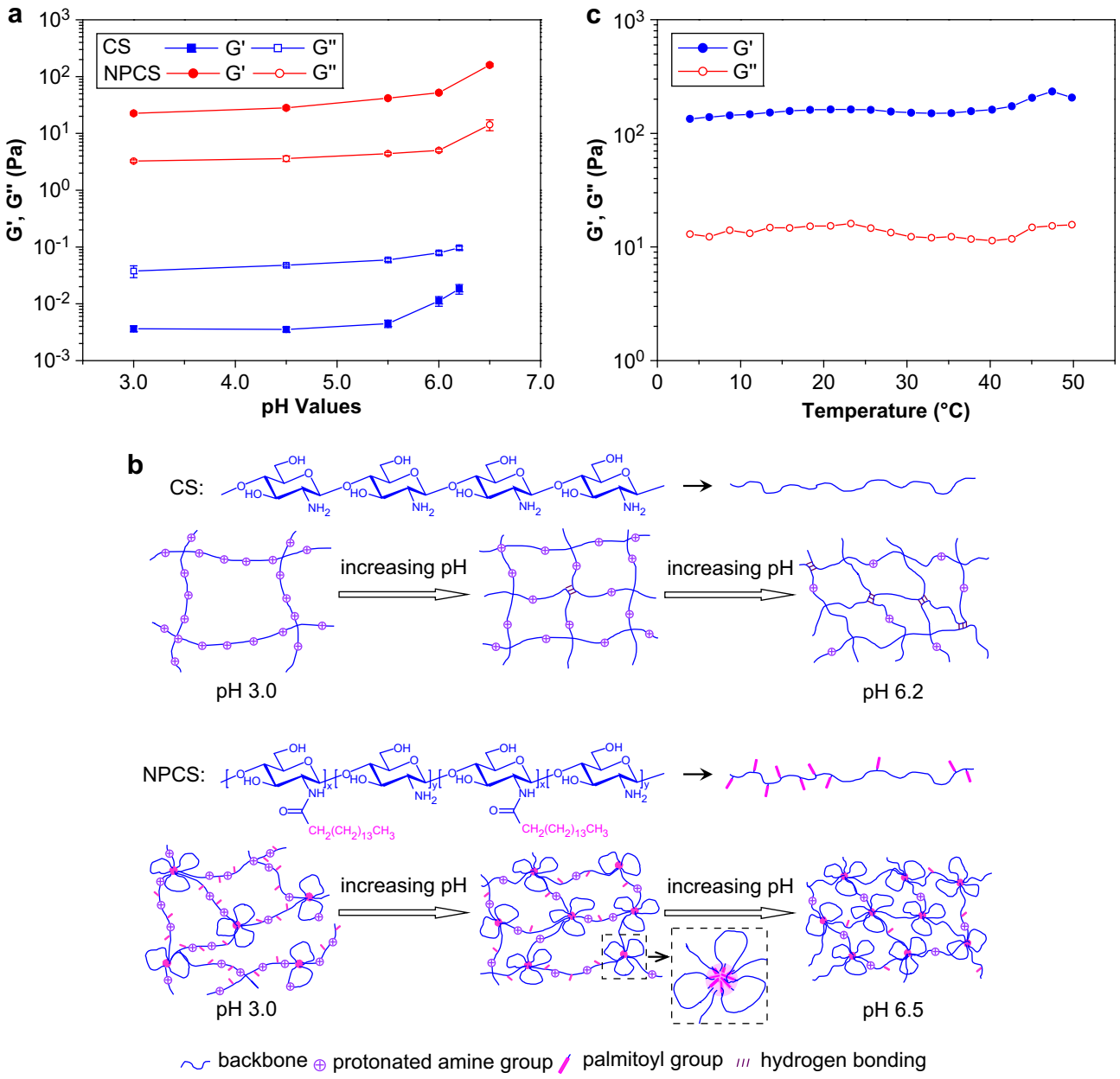

Fig. 3. (a) Elastic (G') and viscous (G'') moduli of aqueous CS (1% w/v) and aqueous NPCS (1% w/v) measured at a constant frequency of 0.1 Hz as a function of pH ($n = 5$); (b) schematic illustrations of the structures of CS and NPCS at different pH environments; (c) dynamic temperature sweeps of aqueous NPCS (1% w/v, pH 6.5) at an oscillatory strain amplitude of 1% and a frequency of 0.1 Hz.

At pH ≦ 6.5, although G' was larger than G'', aqueous NPCS was really a structured fluid, as it flowed almost as liquids at large deformations [34]. When aqueous NPCS was subjected to a shear, its physical cross-links between polymer chains might be ruptured. Fig. 4a clearly showed that the viscosity of aqueous NPCS (at pH 6.5) decreased significantly with increasing the shear rate subjected, a shear-thinning behavior. This drop in viscosity (shear thinning) resulted from the disruption of the physical cross-links between NPCS polymers by the application of strains, suggesting that aqueous NPCS might be able to squeeze through the channel of a needle.

Importantly, aqueous NPCS was capable of quickly reforming after the cessation of shearing due to a quick molecular self-association process. In Fig. 4b, a time sweep experiment was immediately performed after the application of 1000% strain on aqueous NPCS for 180 s. As shown, the elastic modulus (G') of aqueous NPCS increased instantly, an indication of a quick recovery of its elastic nature, as a result of the restoration of their disrupted physical cross-links. The subsequent quick recovery of its elastic nature might render aqueous NPCS the capability of avoiding diffusion into its surrounding environment. In clinical applications, fast hydrogelation is desired to prevent diffusion of hydrogel precursors or bioactive molecules/cells to the surrounding tissue [9,10]. The aforementioned results indicated that aqueous NPCS is a shear-thinning fluid and exhibits a quick recovery of its elastic properties after shearing is ended (Fig. 4c).

3.3. Hydrogel strength

Fig. 5 displayed the elastic modulus (G') of NPCS measured at a constant frequency of 0.1 Hz as functions of pH and ionic strength. As shown, the elastic modulus of NPCS (in the absence of

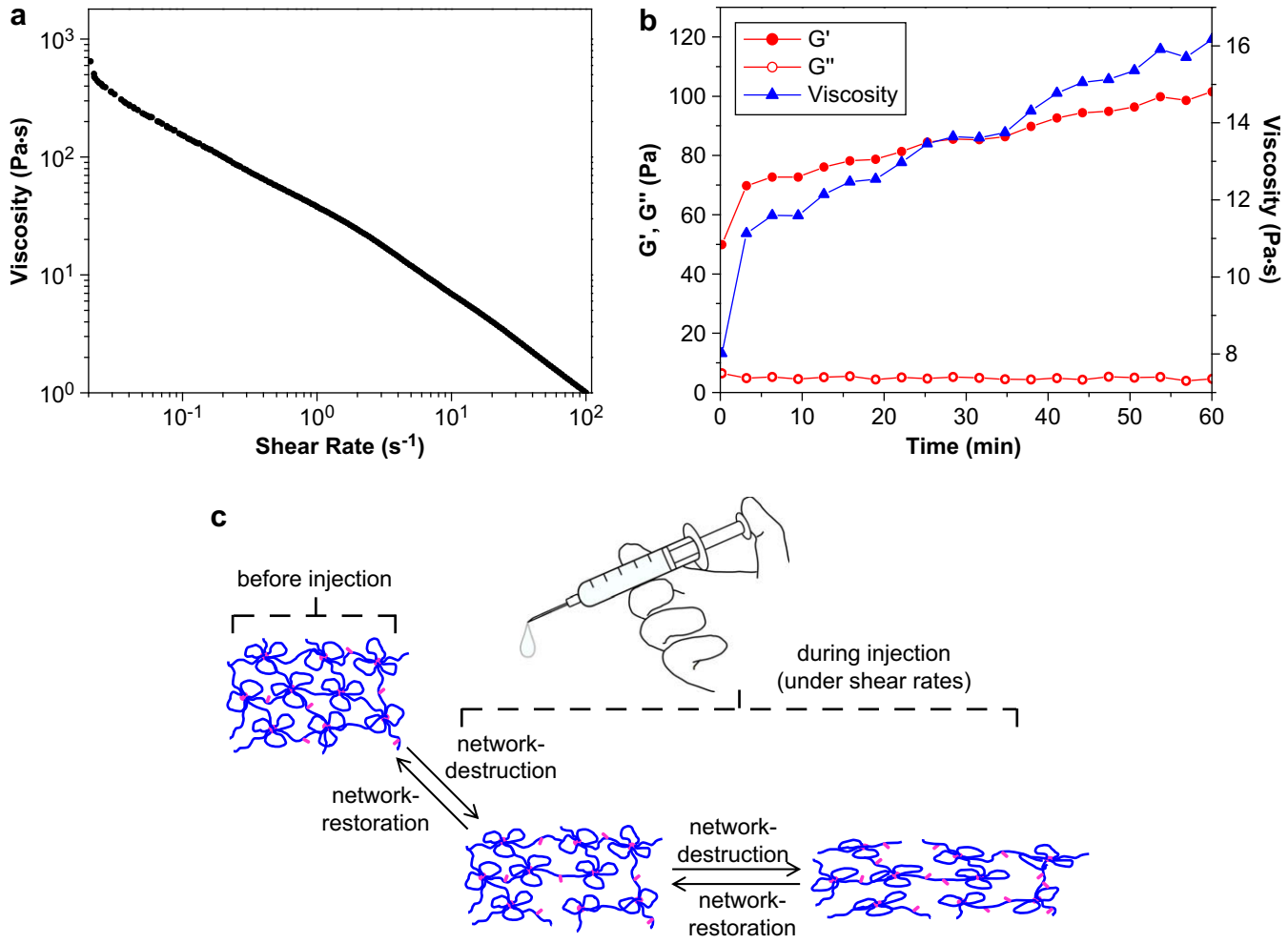

Fig. 4. (a) Rate sweep data of aqueous NPCS (1% w/v, pH 6.5) indicative of shear-thinning behavior; (b) restoration of elastic modulus (G') and viscosity of aqueous NPCS (1% w/v, pH 6.5) as a function of time after the cessation of strain treatment (1000% strain for 180 s); (c) schematic illustrations of the destruction of physical cross-links between NPCS polymers by the application of strain and the quick restoration of their physical cross-links after shearing is ended.

environmental ions, without ionic strength) increased dramatically with increasing pH, presumably due to a significance increase in its extent of physical cross-links. As an example, when pH was raised from 6.5 to 7.0, NPCS showed a drastic increase in G' by about an order of magnitude and the material was in the form of hydrogel as it responded as a solid even under large shear rates ($G' > 1$ kPa) [34,35]. These results suggested that the transition between aqueous NPCS and its resulted hydrogel occurred within a narrow pH range (pH 6.5–7.0).

In the presence of environmental ions (NaCl, with ionic strength), the hydrogel strength (G') of NPCS increased significantly ($P < 0.05$), particularly at low pH. This is because the electrostatic repulsion resulting from the charged groups ($-NH_3^+$) on NPCS was suppressed appreciably by the accumulation of counterions diffused from the environment (the screening effect) [36], thus increasing their hydrophobic interaction (Fig. 5b). With increasing pH, the amount of the protonated amine groups decreased notably, and thus this screening effect became less important. Up to an ionic strength of 0.15 M, the strength of NPCS hydrogel did not increase any more, because of the saturation of counterions surrounding the protonated amine groups on NPCS. At the physiological environment (pH 7.4, ionic strength 0.15 M), NPCS appeared to be a robust hydrogel, as indicated by its relatively high G' (~27 kPa).

3.4. Structure of hydrogel

The change in supramolecular structure associated with the pH-triggered hydrogelation of NPCS was examined by SAXS. Fig. 6a shows the logarithmic plots of the SAXS profiles of CS and NPCS at pH 3.0 and 7.4. The SAXS intensity of CS at pH 3.0 exhibited a power-law dependence of q^{-1} in the high-q region ($q > 0.8$ nm^{-1}), indicating the existence of locally rodlike structure in solution [37,38]. The rodlike entity corresponded to the sections of the cationic CS backbone, which were extended resulting from the charge repulsion. The intensity showed a slight drop toward the lower-q region at $q < 0.7$ nm^{-1} due to the electrostatic repulsion between the positively charged rodlike segments of CS [39].

The scattering intensity of NPCS at pH 3.0 also displayed the q^{-1} dependence at high q but it showed an upturn (with the power-law dependence of $q^{-2.7}$) in the lower-q region ($q < 0.4$ nm^{-1}). The scattering pattern indicated the formation of global network aggregates with the mass fractal dimension of 2.7 [12,38]. The NPCS sub-chains between the crosslinking points in the network were essentially rodlike, thereby leading to the q^{-1} dependence of the high-q intensity [12,38]. At low enough pH (pH < 4.0), the polymer charge saturated to its maximal value such that only a limited fraction of the hydrophobic side chains associated locally to form

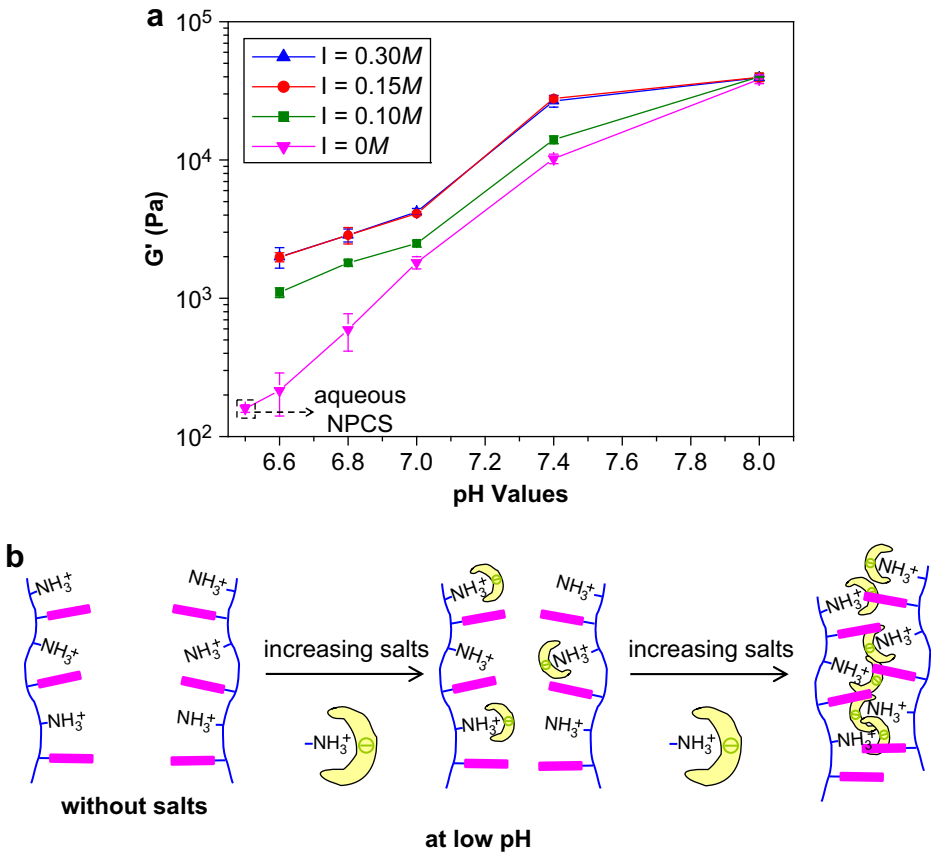

Fig. 5. (a) Elastic modulus (G') of NPCS hydrogel measured at a constant frequency of 0.1 Hz as functions of pH and ionic strength ($n = 5$); (b) schematic illustrations of the hydrogel strength of NPCS in the presence of environmental salts at low pH.

the physical cross-links that tied the polymer chains to form network aggregates.

As pH increased, the charge density along the polymer chain gradually diminished and the reduction in electrostatic repulsion contributed to reinforce the hydrogen bonding between CS and the hydrophobic association in NPCS. At sufficiently high pH, the amine groups of CS became deprotonated and the polymer precipitated due to loss of charge. Fig. 6a also shows the SAXS profile of the CS precipitate (suspended in the aqueous medium) formed at pH 7.4. It can be seen that the SAXS intensity showed a power-law dependence of $q^{-2.4}$ over nearly the entire q region until it transformed to the q^{-1} dependence in the tail region ($q > 2.3$ nm^{-1}). The scattering feature suggested that CS within the precipitate formed the network aggregates with the mass fractal dimension of 2.4. The fact that the q^{-1} power law emerged at much higher q (compared with the case of NPCS at pH 3.0) attested that the rodlike sub-chains between the physical cross-links in the network were much shorter because the network had a high number density of the cross-links due to severe aggregation of CS chains.

The scattering profile of NPCS hydrogel formed at pH 7.4 displayed different features from that of CS, as a small peak located at 2.0 nm^{-1} was discernible. In this case, the strong hydrophobic interaction between the side chains should cause the polymer chains to aggregate severely. A nanophase separation between the CS backbone and the palmitoyl side chains driven by their polar–nonpolar repulsion took place within the aggregates, and the characteristic spacing of ca. 3 nm between the nanodomains thus formed yielded a peak in the SAXS profile [40,41]. The nanophase-separated morphology was further confirmed by the TEM micrograph in Fig. 6b showing the real-space morphology of the NPCS hydrogel. It can be seen that the nanophase separation led to the formation of a network or sponge structure, characterized by the extensive interconnection of the nanodomains consisting of the side chains (the bright regions in the TEM micrograph) or the backbone (the dark regions). The nanodomain spacings were found to be around 3–5 nm, in agreement with that deduced from the SAXS peak.

Our SAXS measurements allowed the structures with the length scale between ca. 60 nm to ca. 2 nm to be probed, and the results revealed that the pH-triggered hydrogelation of NPCS was accompanied with the transformation of the nanostructure from a network aggregate to a nanophase-separated sponge structure due to the dominance of hydrophobic interaction near physiological pH. Because the hydrogelation process may sometimes involve the formation of characteristic structures at multiple length scales, we also examined the morphology of NPCS hydrogels at a more global scale by SEM to establish the hierarchical structure of the hydrogels as well as the hydrogelation mechanism. Fig. 6b shows the SEM micrograph of the hydrogel imaged after removing water by lyophilization. A network structure with the interconnected macrodomains comprising of the polymer and the pores originally occupied by water was observed. The sizes of the pores were around 10–20 μm.

The SEM micrograph along with the SAXS/TEM results disclosed the occurrence of two levels of phase separation upon the pH-triggered hydrogelation of NPCS, namely, a macrophase separation between NPCS and water that led to the formation of micrometer-sized interconnected NPCS-macrodomains and water-macrodomains (as revealed by SEM), and a nanophase separation between the backbone and side chains of NPCS within

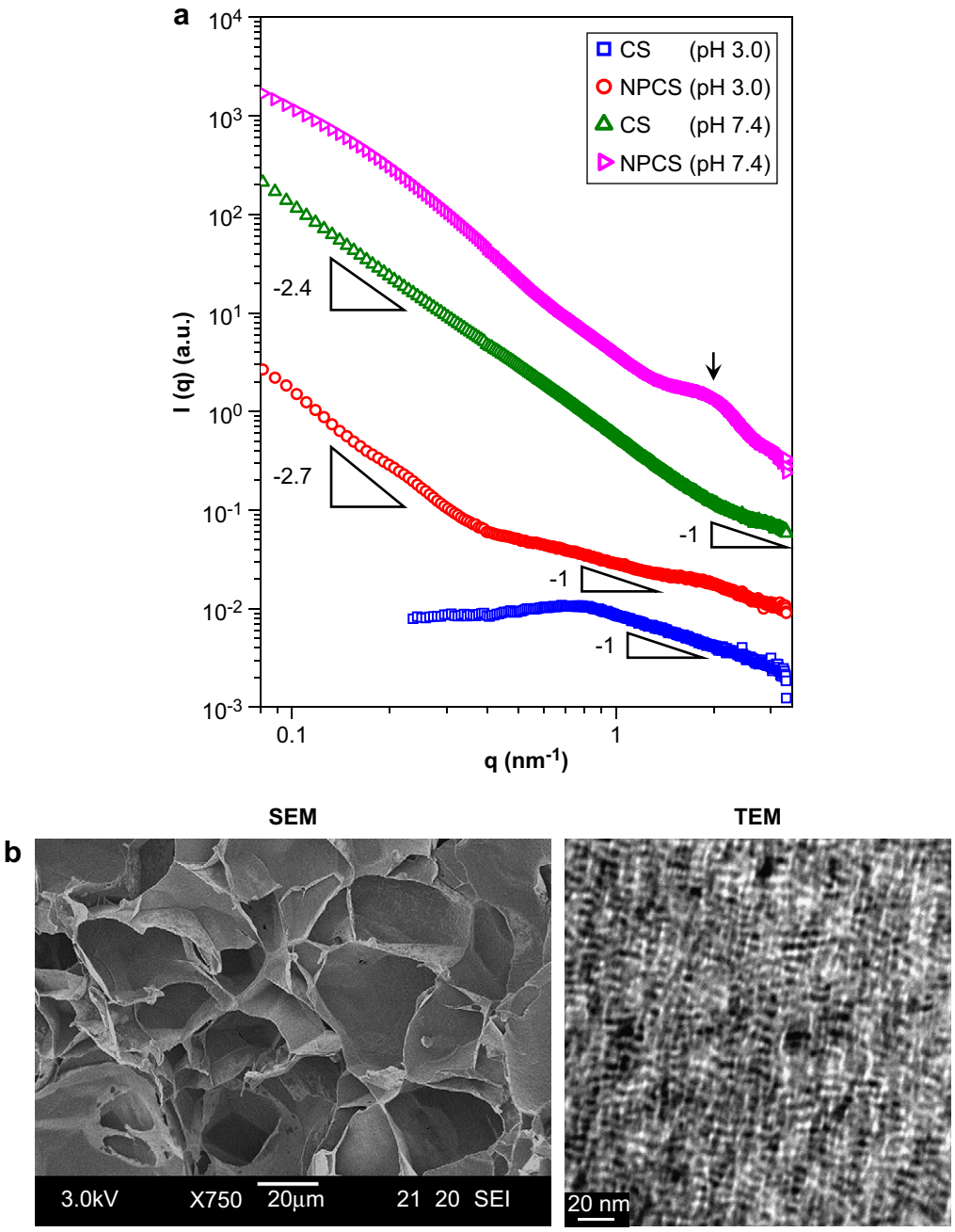

Fig. 6. (a) Small-angle X-ray scattering (SAXS) profiles in log–log plots of CS and NPCS obtained at pH 3.0 and pH 7.4; (b) SEM and TEM micrographs of NPCS hydrogel obtained at pH 7.4.

the NPCS-macrodomains (as shown by SAXS and TEM). We thus proposed that the hydrogelation was driven by a macrophase separation at the higher pH; in the course of the phase separation, the regions that enriched NPCS started to develop a nanophase separation once the polymer concentration exceeded a certain threshold value, leading to the formation of an interconnected sponge nanostructure. The connectivity between the nanodomains thus formed spread over a long range and effectively immobilized the NPCS-macrodomains, thereby preventing the system from attaining the equilibrium phase-separated morphology by the coarsening process. As a result, the phase-separated structure with extensive connectivity of NPCS-macrodomains was arrested such that the system attainted the hydrogel property.

3.5. Hydrogel formation

The pH of body fluids that bath cells and tissues is maintained within a narrow range (~pH 7.4) [42]. During injection, it was noted that aqueous NPCS (hydrogel precursor) was readily squeezed through the channel of the needle. As shown in Fig. 7a, immediately after the injected droplet of aqueous NPCS (pH 6.5) was in contact with saline (pH 7.4), a semi-transparent bead was instantly produced; no apparent diffusion of NPCS in saline was observed. This is because upon contacting with saline, the hydrophobic interaction of palmitoyl groups at the most outer layer of NPCS droplets became dominant instantly (i.e., a significant increase in physical cross-links), thereby transforming NPCS composing of inter-chain network aggregates into a hydrogel layer

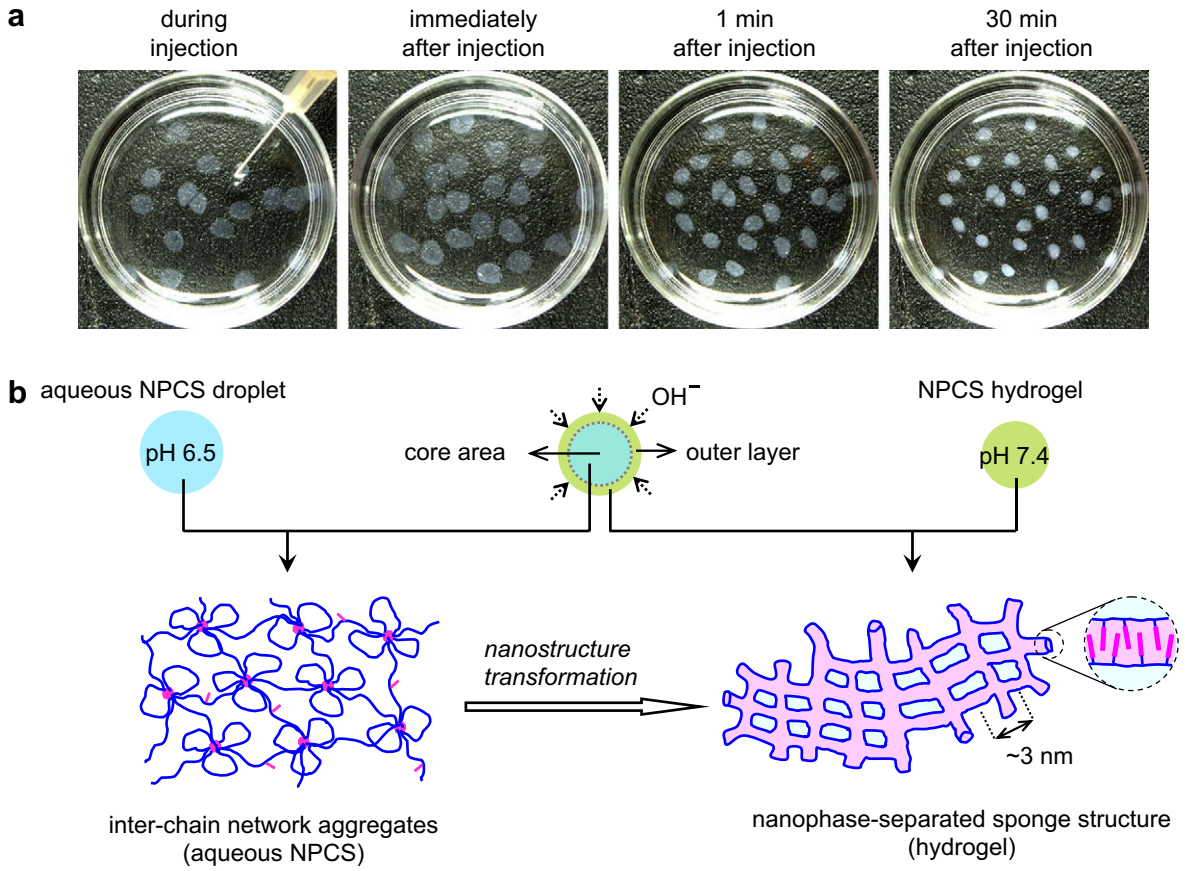

Fig. 7. (a) Time courses of photographs of aqueous NPCS at pH 6.5 after injection through a needle into a physiological saline solution (pH 7.4) at 37 °C; (b) schematic illustrations of changes in structure with time associated with the hydrogelation of NPCS triggered by its environmental pH.

in a sponge structure. At this moment in time, the pH in the core area of the bead was still approximately pH 6.5.

With time increasing, this bead shrank relatively and became opaque. As schematically illustrated in Fig. 7b, OH^- in the surrounding fluid diffused into the core of the bead gradually (i.e., the pH value of the bead became neutral from the surface to the center step by step), thus increasing the physical cross-links within the entire bead. Additionally, premature hydrogelation inside the delivery vehicle was not observed, since the pH of hydrogel precursors inside the needle would not be affected by their surrounding fluid. This is another significant advantage of the present pH-sensitive hydrogel over the temperature-sensitive systems.

3.6. *In vitro cytotoxicity*

Fig. 8a shows photomicrographs of the cells cultured in the media treated with extracts of CS precipitates or NPCS hydrogels. Calcein-AM hydrolysis in live cells produces a green fluorescent signal while ethidium homodimer is excluded from live cells and produces a red fluorescent signal only in dead cells [18]. Live/dead staining demonstrated that most of the cells cultured in different test media were viable. The total viable cells for all studied groups were found to be comparable ($P > 0.05$), determined by the optical density readings obtained in the MTT assay (Fig. 8b). These results indicated that there was no significant toxicity for CS precipitates and NPCS hydrogels.

3.7. *In vivo biocompatibility and degradability*

In the *in vivo* biocompatibility study, aqueous NPCS (pH 6.5) was injected through a needle into the subcutaneous space of a rat model. Thirty minutes after injection, a massive hydrogel in one piece was found at the location of subcutaneous injection. The hydrogel implanted subcutaneously could be readily isolated using a pair of tweezers (Fig. 1). Optical photomicrographs of histological sections of the hydrogel and its surrounding tissue retrieved at 2 and 6 weeks after implantation are shown in Fig. 9a. At 2 weeks post implantation, a relatively large number of inflammatory cells were observed at interfaces of the tissue and the hydrogel (area a in Fig. 9a). Additionally, there were some inflammatory cells infiltrating into the outer layer of the hydrogel (area b).

The inflammatory cells were identified by immunohistochemical staining using a CD68 antibody that can recognize the antigen expressed by macrophages [43]. The stained sections were counterstained with PI to mark the position of cell nuclei. As shown in Fig. 9b (area a), CD68-positive cells were observed in the vicinity of the implanted hydrogel. These data showed that subcutaneous injection of the hydrogel resulted in an ongoing foreign body reaction characterized by the infiltration of macrophages [7,44,45]. At 6 weeks after implantation, the inflammatory reaction surrounding the hydrogel was observed to subside, together with a noticeable reduction in the number of CD68-positive cells (area A in Fig. 9a and b). A decrease in the number of macrophages (inflammation-mediating cells) prevented progression to the chronic inflammatory phase; a mild tissue response *in vivo* was thus observed.

In vivo degradation of the implanted hydrogel was also investigated in this study. At 2 weeks after implantation, a fractured structure at the outer layer of the hydrogel (stained in green due to the autofluorescence nature of CS) was

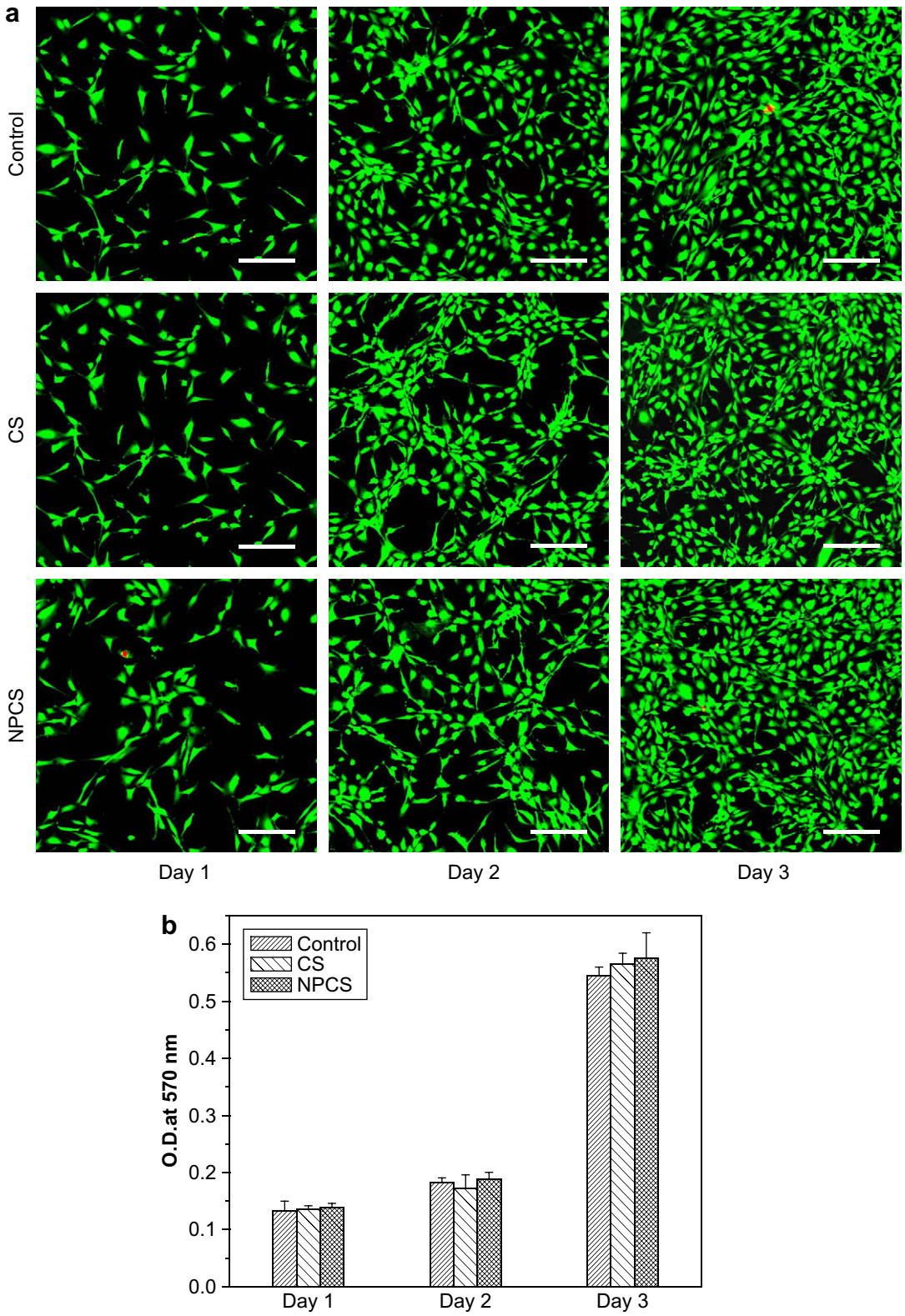

Fig. 8. (a) Photomicrographs (scale bars, 200 μm) and (b) optical density readings (obtained in the MTT assay, $n = 5$) of the cells cultured in the media treated with extracts of CS precipitates or NPCS hydrogels for distinct durations. The fresh medium was used as a control (Control).

observed. After 6 weeks, the hydrogel was extensively degraded and cells migrated into deeper parts of the hydrogel. It is well known that CS is degraded by enzymatic hydrolysis *in vivo*; the primary enzyme is lysozyme which appears to target acetylated residues [46]. Macrophages are the predominant cell type in the tissue reaction to the polymer devices; they play an essential role in phagocytosis of the polymer and its degradation.

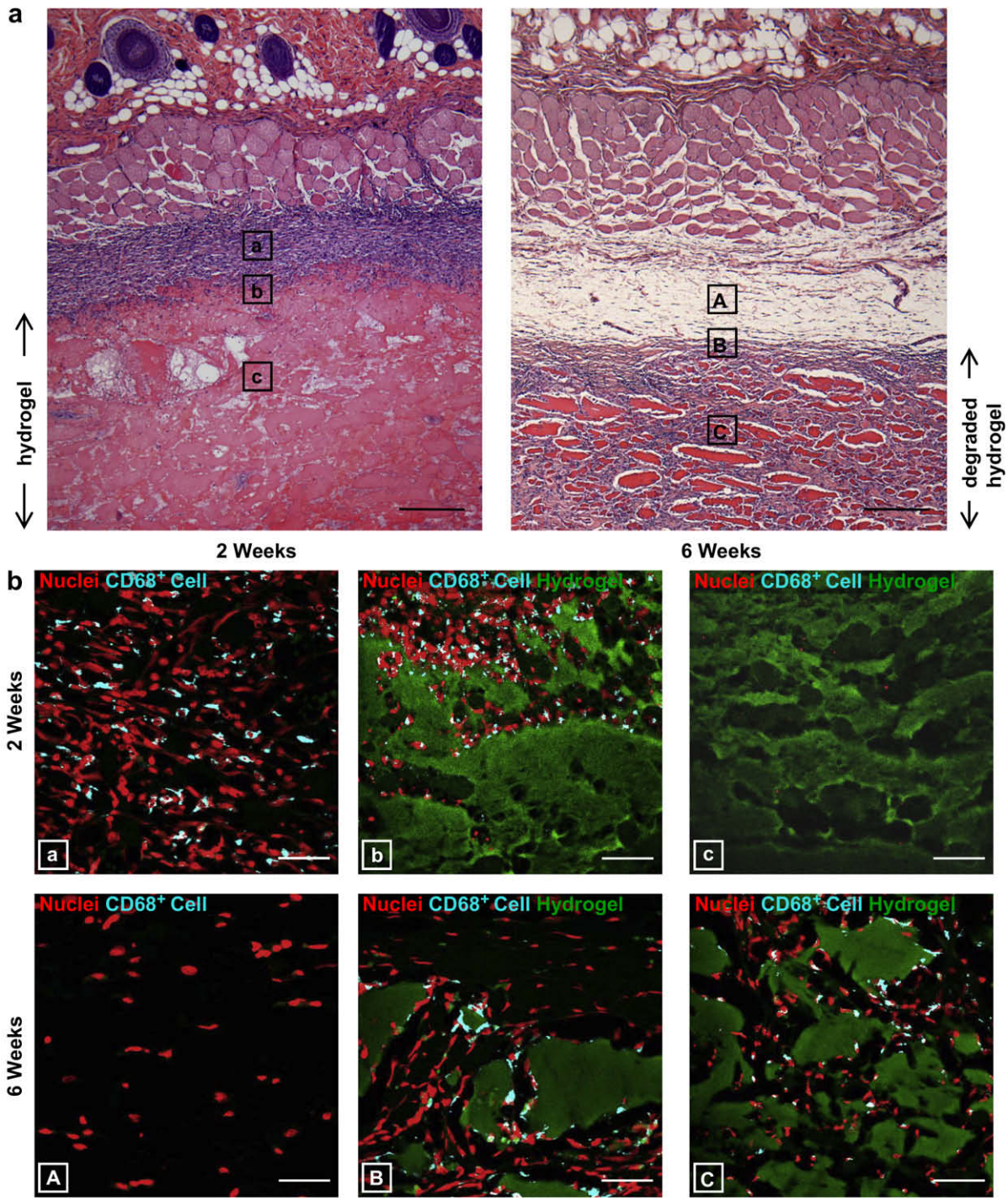

Fig. 9. (a) Optical photomicrographs of histological sections (scale bars, 250 μm) and (b) CLSM images (scale bars, 40 μm) of the hydrogel and its surrounding tissue retrieved at 2 and 6 weeks after implantation.

4. Conclusions

In this study, we successfully developed an *in-situ* forming hydrogel made of aqueous NPCS, an associating polyelectrolyte. Through a proper balance between charge repulsion and hydrophobic interaction, aqueous NPCS could undergo a rapid hydrogelation triggered simply by its environmental pH within a narrow range. The *in vitro* results indicated that this NPCS hydrogel was nontoxic. In a rat subcutaneous model, the hydrogel was found to be degradable and was associated with an initial macrophage response which decreased with time as the degradation proceeded. These results suggested that the developed NPCS hydrogel may be useful for biomedical applications.

Acknowledgment

This work was supported by a grant from the National Science Council (NSC 97-2120-M-007-001), Taiwan, Republic of China. The synchrotron X-ray scattering experiment supported by the NSRRC under Project ID 2007-1-018-3 was gratefully acknowledged.

Appendix

Figures with essential color discrimination. The majority of the figures in this article have parts that may be difficult to interpret in black and white. The full color images can be found in the on-line version, at doi:10.1016/j.biomaterials.2009.05.052.

References

[1] Lee KY, Yuk SH. Polymeric protein delivery systems. Prog Polym Sci 2007;32:669–97.
[2] Chaterji S, Kwon IK, Park K. Smart polymeric gels: redefining the limits of biomedical devices. Prog Polym Sci 2007;32:1083–122.
[3] Yu L, Ding J. Injectable hydrogels as unique biomedical materials. Chem Soc Rev 2008;37:1473–81.
[4] Jin R, Teixeira LSM, Dijkstra PJ, Karperien M, Blitterswijk CA, Zhong ZY, et al. Injectable chitosan-based hydrogels for cartilage tissue engineering. Biomaterials 2009;30:2544–51.
[5] Jeong B, Kim SW, Bae YH. Thermosensitive sol–gel reversible hydrogels. Adv Drug Deliv Rev 2002;54:37–51.
[6] Yeo Y, Highley CB, Bellas E, Ito T, Marini R, Langer R, et al. *In situ* cross-linkable hyaluronic acid hydrogels prevent post-operative abdominal adhesions in a rabbit model. Biomaterials 2006;27:4698–705.
[7] Shim WS, Kim JH, Park H, Kim K, Kwon IC, Lee DS. Biodegradability and biocompatibility of a pH- and thermo-sensitive hydrogel formed from a sulfonamide-modified poly(ε-caprolactone-co-lactide)–poly(ethylene glycol)–poly(ε-caprolactone-co-lactide) block copolymer. Biomaterials 2006;27:5178–85.
[8] Suh JM, Bae SJ, Jeong B. Thermogelling multiblock poloxamer aqueous solutions with closed-loop sol–gel–sol transition upon increasing pH. Adv Mater 2005;17:118–20.
[9] Hiemstra C, Zhou W, Zhong Z, Wouters M, Feijen J. Rapidly *in situ* forming biodegradable robust hydrogels by combining stereocomplexation and photopolymerization. J Am Chem Soc 2007;129:9918–26.
[10] Choi HS, Huh KM, Ooya T, Yui N. pH- and thermosensitive supramolecular assembling system: rapidly responsive properties of β-cyclodextrin-conjugated poly(ε-lysine). J Am Chem Soc 2003;125:6350–1.
[11] Rinaudo M. Chitin and chitosan: properties and applications. Prog Polym Sci 2006;31:603–32.
[12] Chiu YL, Chen MC, Chen CY, Lee PW, Mi FL, Jeng US, et al. Rapidly *in situ* forming hydrophobically-modified chitosan hydrogels *via* pH-responsive nanostructure transformation. Soft Matter 2009;5:962–5.
[13] Curotto E, Aros F. Quantitative determination of chitosan and the percentage of free amino groups. Anal Biochem 1993;211:240–1.
[14] Tôei K, Kohara T. A conductometric method for colloid titrations. Anal Chim Acta 1976;83:59–65.
[15] Sawyer LC, Grubb D. Polymer microscopy. 2nd ed. London: Chapman & Hall; 1996.
[16] Alt V, Bechert T, Steinrücke P, Wagener M, Seidel P, Dingeldein E, et al. An *in vitro* assessment of the antibacterial properties and cytotoxicity of nanoparticulate silver bone cement. Biomaterials 2004;25:4383–91.
[17] Loh XJ, Sng KBC, Li J. Synthesis and water-swelling of thermo-responsive poly(ester urethane)s containing poly(ε-caprolactone), poly(ethylene glycol) and polypropylene glycol. Biomaterials 2008;29:3185–94.
[18] Kretsinger JK, Haines LA, Ozbas B, Pochan DJ, Schneider JP. Cytocompatibility of self-assembled β-hairpin peptide hydrogel surfaces. Biomaterials 2005;26:5177–86.
[19] Yang TF, Chen CN, Chen MC, Lai CH, Liang HF, Sung HW. Shell-crosslinked pluronic L121 micelles as a drug delivery vehicle. Biomaterials 2007;28:725–34.
[20] Tien CL, Lacroix M, Ispas-Szabo P, Mateescu MA. *N*-acylated chitosan: hydrophobic matrices for controlled drug release. J Control Release 2003;93:1–13.
[21] Liang G, Jia-Bi Z, Fei X, Bin N. Preparation, characterization and pharmacokinetics of *N*-palmitoyl chitosan anchored docetaxel liposomes. J Pharm Pharmacol 2007;59:661–7.
[22] Han J, Guenier AS, Salmieri S, Lacroix M. Alginate and chitosan functionalization for micronutrient encapsulation. J Agric Food Chem 2008;56:2528–35.
[23] Kumar MNVR, Muzzarelli RAA, Muzzarelli C, Sashiwa H, Domb AJ. Chitosan chemistry and pharmaceutical perspectives. Chem Rev 2004;104:6017–84.
[24] Wade LG. Organic chemistry. 6th ed. Upper Saddle River, NJ: Pearson Prentice Hall; 2006.
[25] Desbrières J, Martinez C, Rinaudo M. Hydrophobic derivatives of chitosan: characterization and rheological behaviour. Int J Biol Macromol 1996;19:21–8.
[26] Kjøniksen AL, Nyström B, Iversen C, Nakken T, Palmgren O, Tande T. Viscosity of dilute aqueous solutions of hydrophobically modified chitosan and its unmodified analogue at different conditions of salt and surfactant concentrations. Langmuir 1997;13:4948–52.
[27] Kjøniksen AL, Iversen C, Nyström B, Nakken T, Palmgren O. Light scattering study of semidilute aqueous systems of chitosan and hydrophobically modified chitosans. Macromolecules 1998;31:8142–8.
[28] Nyström B, Kjøniksen AL, Iversen C. Characterization of association phenomena in aqueous systems of chitosan of different hydrophobicity. Adv Colloid Interface Sci 1999;79:81–103.
[29] Esquenet C, Buhler E. Phase behavior of associating polyelectrolyte polysaccharides. 1. Aggregation process in dilute solution. Macromolecules 2001;34:5287–94.
[30] Esquenet C, Terech P, Boué F, Buhler E. Structural and rheological properties of hydrophobically modified polysaccharide associative networks. Langmuir 2004;20:3583–92.
[31] Yue TW, Chien WC, Tseng SJ, Tang SC. EDC/NHS-mediated heparinization of small intestinal submucosa for recombinant adeno-associated virus serotype 2 binding and transduction. Biomaterials 2007;28:2350–7.
[32] Kötz J, Kosmella S, Beitz T. Self-assembled polyelectrolyte systems. Prog Polym Sci 2001;26:1199–232.
[33] Yi H, Wu LQ, Bentley WE, Ghodssi R, Rubloff GW, Culver JN, et al. Biofabrication with chitosan. Biomacromolecules 2005;6:2881–94.
[34] Kavanagh GM, Ross-Murphy SB. Rheological characterization of polymer gels. Prog Polym Sci 1998;23:533–62.
[35] Schneider JP, Pochan DJ, Ozbas B, Rajagopal K, Pakstis L, Kretsinger J. Responsive hydrogels from the intramolecular folding and self-assembly of a designed peptide. J Am Chem Soc 2002;124:15030–7.
[36] Petrache HI, Zemb T, Belloni L, Parsegian VA. Salt screening and specific ion adsorption determine neutral-lipid membrane interactions. Proc Natl Acad Sci U S A 2006;103:7982–7.
[37] Roe RJ. Methods of X-ray and neutron scattering in polymer science. New York: Oxford University Press; 2000.
[38] Li YC, Chen KB, Chen HL, Hsu CS, Tsao CS, Chen JH, et al. Fractal aggregates of conjugated polymer in solution state. Langmuir 2006;22:11009–15.
[39] Nishida K, Kaji K, Kanaya T, Shibano T. Added salt effect on the intermolecular correlation in flexible polyelectrolyte solutions: small-angle scattering study. Macromolecules 2002;35:4084–9.
[40] Beiner M, Huth H. Nanophase separation and hindered glass transition in side-chain polymers. Nat Mater 2003;2:595–9.
[41] Floudas G, Štepánek P. Structure and dynamics of poly(*n*-decyl methacrylate) below and above the glass transition. Macromolecules 1998;31:6951–7.
[42] Mader SS, Pendarvis MP. Biology. 9th ed. Dubuque, IA: McGraw-Hill Higher Education; 2007.
[43] Chen CH, Chang Y, Wang CC, Huang CH, Huang CC, Yeh YC, et al. Construction and characterization of fragmented mesenchymal-stem-cell for intramuscular injection. Biomaterials 2007;28:4643–51.
[44] Mi FL, Tan YC, Liang HF, Sung HW. In vivo biocompatibility and degradability of a novel injectable-chitosan-based implant. Biomaterials 2002;23:181–91.
[45] Wang HJ, Gong SJ, Lin ZX, Fu JX, Xue ST, Huang JC, et al. *In vivo* biocompatibility and mechanical properties of porous zein scaffolds. Biomaterials 2007;28:3952–64.
[46] Hirano S, Tsuchida H, Nagao N. *N*-Acetylation in chitosan and the rate of its enzymic hydrolysis. Biomaterials 1989;10:574–6.